Proceedings of the ASME 2013 International Design Engineering Technical Conferences & Computers and Information in Engineering Conference
IDETC/CIE 2013
August 4-7, 2013, Portland, OR, USA

DETC2013-12809.

MULTI-OBJECTIVE OPTIMIZATION OF A DISC BRAKE SYSTEM BY USING SPEA2 AND RBFN

Kaveh Amouzgar
Asim Rashid
Niclas Stromberg
Department of Mechanical Engineering,
School of Engineering, Jönköping University,
P.O. Box 1026, SE-551 11 Jönköping
Tel: +46 (0)36 101627, Fax: +46 (0)36 125331
Email: Kaveh.Amouzgar@jth.hj.se,
Asim.Rashid@jth.hj.se,
Niclas.Stromberg@jth.hj.se.

ABSTRACT

Many engineering design optimization problems involve multiple conflicting objectives, which today often are obtained by computational expensive finite element simulations. Evolutionary multi-objective optimization (EMO) methods based on surrogate modeling is one approach of solving this class of problems. In this paper, multi-objective optimization of a disc brake system to a heavy truck by using EMO and radial basis function networks (RBFN) is presented. Three conflicting objectives are considered. These are: 1) minimizing the maximum temperature of the disc brake, 2) maximizing the brake energy of the system and 3) minimizing the mass of the back plate of the brake pad. An iterative Latin hypercube sampling method is used to construct the design of experiments (DoE) for the design variables. Next, thermo-mechanical finite element analysis of the disc brake, including frictional heating between the pad and the disc, is performed in order to determine the values of the first two objectives for the DoE. Surrogate models for the maximum temperature and the brake energy are created using RBFN with polynomial biases. Different radial basis functions are compared using statistical errors and cross validation errors (PRESS) to evaluate the accuracy of the surrogate models and to select the most accurate radial basis function. The multi-objective optimization problem is then solved by employing EMO using the strength Pareto evolutionary algorithm (SPEA2). Finally, the Pareto fronts generated by the proposed methodology are presented and discussed.

INTRODUCTION

Disc brakes are used to stop or adjust the speed of a vehicle by pressing a set of pads against a rotating disc. It converts the kinetic energy of the moving vehicle mainly into heat. This heat causes the disc-pad interface temperature to rise in a short period of time. The high temperature can cause buckling, phase transformation (in case of cast iron) [1] or fatigue cracks on a disc surface [2]. At higher temperatures, pad materials can suffer loss in performance due to fade [3] and also wear faster [4]. Therefore it is desired to keep the disc and pad surface temperatures at minimum. At the same time, it is also desired to maximize brake energy; energy converted into heat during a brake application for a given time.

It has been shown that only a portion of a pad is in actual contact with the disc and contact pressure distribution is not uniform on the pad surface [5]. The regions where contact pressure is higher generates more heat which results in higher temperature in those regions. There are many factors affecting the contact

pressure distribution e.g. thermomechanical deformations, wear history and elastic properties of pad. One way to reduce the maximum temperature is to make the contact pressure distribution relatively uniform. The contact pressure distribution is strongly influenced by the back plate of the pad.

Optimization of a real world application most often consists of more than one objective and in engineering problems these objectives are usually conflicting. In such case, one extreme solution would not satisfy both objective functions and the optimal solution of one objective will not necessary be the best solution for the other objective(s). Therefore different solutions will produce trade-off between different objectives and a set of solutions is required to represent the optimal solutions of all objectives. The characteristic of evolutionary optimization methods which uses a population of solutions that evolve in each generation is well suited for multi-objective optimization problems. The most representative, discussed and compared evolutionary algorithms are non-dominated sorting genetic algorithm (NSGA-II) [6], strength Pareto evolutionary algorithm (SPEA, SPEA2) [7,8], Pareto archived evolution strategy (PAES) [9,10], and Pareto enveloped based selection algorithm (PESA, PESA II) [11,12]. Extensive comparison studies and numerical simulation on various test problems conclude to a better overall behavior of NSGA-II and SPEA2 compared to the other algorithms. In this study the SPEA2 has been used to optimize the three objectives, since it seems to indicate some advantages over NSGA-II where more than two objectives are present.

Mutli-objective optimization of an engineering problem requires several evaluations of each objective within the design space leading to thousands or millions of simulation runs. Depending on the complexity of the problem each could entail hours of computation time to find a set of optimal solutions. Therefore, coupling computational tools with mathematical procedures or algorithms for design optimization is practically difficult and computationally expensive. To remedy this issue, metamodels or surrogates approaches are employed. The basic idea of metamodeling is to create an approximation function of the real model in some sampling points within the design space. This procedure is usually called training or fitting the metamodel. The sampling points are determined using different strategies with the main objective of filling the entire design space such as factorial design, Latin hypercube, etc.

Several metamodeling techniques exists and are used by researchers and engineers such as response surface methodology [13], Kriging [14], radial basis function networks (RBFN) [15], support vector regression (SVR) [16] and artificial neural networks [17]. Despite the numerous studies comparing different metamodeling techniques, there is no one joint belief in dominance of one method over others. In all comparison studies benchmarks and test problems are employed to compare the results of different techniques, which in result it can be argued that a real engineering application may be totally different from the benchmarks. Moreover, a number of parameters influences the choice of an accurate method such as non-linearity, number of variables, associated sampling technique, internal parameter setting of each method and number of objectives in optimization problems [18]. In this paper, we intend to use the RBFN with a priori known polynomial biases.

DISC BRAKE SIMULATION

The traditional way to simulate frictional heating of disc brakes is to use the Lagrangian approach in which the finite element mesh of a disc rotates relative to a brake pad. Although this approach works well, it takes extremely long computational times. For optimization studies of brakes this approach is of little importance for practical use. Benseddiq et al. [19] performed an optimization study of brake pads but they used only a two-dimensional FE model, which although reduces the computational time considerably but is not sufficient to model complex behaviour. The rotational symmetry of the disc makes it possible to model it using an Eulerian approach, in which the finite element mesh of the disc does not rotate relative to the brake pad but the material flows through the mesh. This requires significantly low computational time as compared to the Lagrangian approach. Figure 1 shows schematically both the Eulerian and Lagrangian approaches.

Recently, Strömberg [20] developed and implemented an Eulerian approach for simulating frictional heating in disc-pad systems. In the present work, a toolbox developed by Strömberg, which is based on this approach is used to perform the frictional heat analysis of a three-dimensional finite element model of the disc-pad system shown in Fig. 2. In this Eulerian approach the contact pressure is not constant, but varies at each time step taking into account the thermomechanical deformations of the disc and the pad. This updated contact pressure information is used to compute heat generation and flow to the contacting bodies at each time step.

The assembly shown in Fig. 2 is a disc brake system of a heavy Volvo truck. The disc is geometrically symmetric about a plane normal to the z-axis. It is assumed that thermomechanical loads applied to the system are symmetric so only half of this assembly is considered for the simulation. The brake pad is supported by a steel plate at the back side. Some detailed geometry of the disc and back plate has been removed to simplify the model as that is not important for this analysis.

As the disc is formulated in Eulerian framework, heat is transported through the mesh by convection. Energy balance in the disc is then governed by

$$\boldsymbol{M}\dot{\boldsymbol{T}} + (\boldsymbol{N} + \boldsymbol{O} + \boldsymbol{R})\boldsymbol{T} = \boldsymbol{Q}_c, \tag{1}$$

where $\boldsymbol{M}$ is the heat capacity matrix, $\boldsymbol{N}$ is the convection matrix,

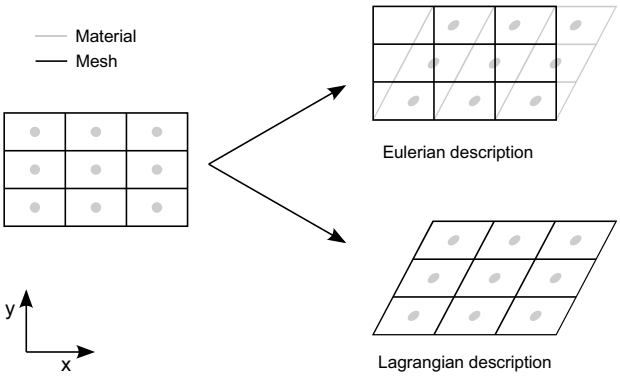

FIGURE 1. SCHEMATIC REPRESENTATION OF EULERIAN AND LAGRANGIAN APPROACH.

$\boldsymbol{O}$ is the conduction matrix, $\boldsymbol{R}$ is the matrix of the artificial conduction to stabilize distortions in the solution caused by nonsymmetric convection matrix in accordance to the streamline-upwind approach, $\boldsymbol{T}$ is a vector of nodal temperature and $\boldsymbol{Q}_c$ is a vector of nodal heat fluxes at the contact surface.

In the analysis linear thermo-elasticity is adopted and equilibrium of the disc is given by

$$\boldsymbol{K}\boldsymbol{d} - \hat{\boldsymbol{K}}\boldsymbol{T} + (\boldsymbol{C}_n + \mu \boldsymbol{C}_t)^T \boldsymbol{P}_n = \boldsymbol{F}_\omega, \tag{2}$$

where $\boldsymbol{d}$ is the displacement vector, $\boldsymbol{K}$ is the stiffness matrix, $\hat{\boldsymbol{K}}$ represents the thermal expansion properties, $\boldsymbol{C}_n$ contains surface normals, $\boldsymbol{C}_t$ defines the tangential sliding directions, μ is the coefficient of friction, $\boldsymbol{P}_n$ contains the normal contact forces at nodes and $\boldsymbol{F}_\omega$ is a vector of centripetal forces.

The normal contact force is assumed to be governed by Signorini's contact conditions and treated by the well known augmented Lagrangian approach, expressed as

$$\boldsymbol{P}_n = \frac{\boldsymbol{P}_n + r\boldsymbol{d}_n + |\, \boldsymbol{P}_n + r\boldsymbol{d}_n \,|}{2}, \tag{3}$$

where $r > 0$ is a penalty coefficient and $\boldsymbol{d}_n = \boldsymbol{C}_n \boldsymbol{d}$.

RADIAL BASIS FUNCTION NETWORKS (RBFN)

Radial basis function networks were originally developed for representing topography based on coordinate data with interpolation [15]. The concept is based on the linear combination of some radial basis functions with weights that are symmetric and centred at each sampling point. The basis functions are expressed in terms of the Euclidean distance of the sampling points $\boldsymbol{x}$ from a center point $\boldsymbol{c}_i$, which typically is taken to be the design

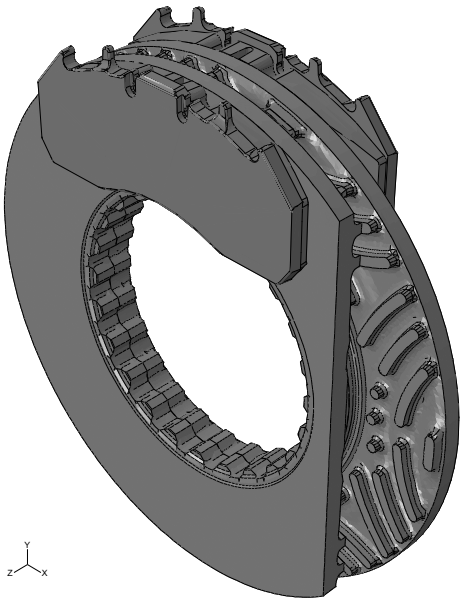

FIGURE 2. THE ASSEMBLY OF THE DISC-PAD SYSTEM.

variable $\hat{\boldsymbol{x}}_i$ at the i_{th} sampling point, in the form of

$$r = ||\boldsymbol{x} - \boldsymbol{c}_i||. \tag{4}$$

The general form of a radial basis function without bias is

$$f(\boldsymbol{x}) = \sum_{i=1}^{n} \lambda_i \phi(r), \tag{5}$$

where n is the number of sampling points, $\phi = \phi(r)$ is a radial basis function, λ_i is the weight for the i_{th} basis function, and $f(\boldsymbol{x})$ is the approximation function. Some of the most commonly used radial basis functions are

$$\begin{aligned} \text{Linear:} \quad & \phi(r) = r, \\ \text{Cubic:} \quad & \phi(r) = r^3, \\ \text{Gaussian:} \quad & \phi(r) = e^{-\gamma r^2},\ 0 \le \gamma \le 1, \\ \text{Quadratic:} \quad & \phi(r) = \sqrt{r^2 + \gamma^2},\ 0 \le \gamma \le 1, \end{aligned} \tag{6}$$

where γ is a positive shape parameter. The classic form of RBFN in Eqn. (5), has been approved inappropriate for linear problems, despites its good performance in highly non-linear problems [21]. Furthemore, the RBFN as in Eqn. (5) might become singular and no interpolation is found. A standard approach

to avoid the aforementioned problems is to augment the classic RBFN with a polynomial bias as

$$f(\boldsymbol{x}) = \sum_{i=1}^{n} \lambda_i \phi(||\boldsymbol{x} - \boldsymbol{c}_i||) + \sum_{j=1}^{m} \beta_j b_j(\boldsymbol{x}), \tag{7}$$

where $b_j = b_j(\boldsymbol{x})$ represents the polynomial basis functions and β_j are the unknown regression coefficients of the polynomial biases. Replacing $\boldsymbol{x}$ and $f(\boldsymbol{x})$ in Eqn. (7) with the n vectors of design variables and corresponding response values leads to the following matrix format:

$$\hat{\boldsymbol{f}} = \boldsymbol{A}\boldsymbol{\lambda} + \boldsymbol{B}\boldsymbol{\beta}, \tag{8}$$

where $\boldsymbol{A}_{i,j} = \phi(||\hat{\boldsymbol{x}}_i - \boldsymbol{c}_j||)$, $\boldsymbol{\lambda} = [\lambda_1, \lambda_2 ... \lambda_n]^T$, $\boldsymbol{B}_{i,j} = b_j(\hat{\boldsymbol{x}}_i)$, $\boldsymbol{\beta} = [\beta_1, \beta_2 ... \beta_m]^T$, and $\hat{\boldsymbol{f}} = \left[\hat{f}_1, \hat{f}_2 ... \hat{f}_n\right]^T$ are the sampling values. Since the unknown parameters are more than the number of equations in Eqn. (8), the equation is undetermined and can not be solved. This is overcome by adding the following orthogonality condition

$$\sum_{i=1}^{n} \lambda_i b_j(\boldsymbol{c}_i) = 0 \quad \text{for } j = 1, 2 ... m. \tag{9}$$

Combining equations (8) and (9) will lead to the matrix form of

$$\begin{bmatrix} \boldsymbol{A} & \boldsymbol{B} \\ \boldsymbol{B}^T & \boldsymbol{0} \end{bmatrix} \begin{Bmatrix} \boldsymbol{\lambda} \\ \boldsymbol{\beta} \end{Bmatrix} = \begin{Bmatrix} \hat{\boldsymbol{f}} \\ \boldsymbol{0} \end{Bmatrix}. \tag{10}$$

The unknown coefficients $\boldsymbol{\lambda}$ and $\boldsymbol{\beta}$ of the RBFN will be obtained by solving Eqn. (10).

The RBFN approach used in this paper is not based on the standard approach presented above with a posteriori bias, but we use instead a priori bias. A parabolic or quadratic response surface is fitted to the sampling points as

$$\begin{aligned} f(\boldsymbol{x}) &= \beta_0 + \sum_{i=1}^{n} \beta_i x_i + \sum_{i=1}^{n} \beta_{ii} x_i^2, \\ f(\boldsymbol{x}) &= \beta_0 + \sum_{i=1}^{n} \beta_i x_i + \sum_{i=1}^{n} \beta_{ii} x_i^2 + \sum_{i=1}^{n-1} \sum_{j=i+1}^{n} \beta_{ij} x_i x_j. \end{aligned} \tag{11}$$

If n vectors of DoEs and their corresponding responses are applied to any of the equations in Eqn. (11), n equations will be obtained which can be expressed in the matrix form as

$$\hat{\boldsymbol{f}} = \boldsymbol{B}\boldsymbol{\beta}, \tag{12}$$

where the matrix of unknown regression coefficients $\boldsymbol{\beta}$ is determined by the normal equation as

$$\hat{\boldsymbol{\beta}} = (\boldsymbol{B}^T \boldsymbol{B})^{-1} (\boldsymbol{B}^T \hat{\boldsymbol{f}}). \tag{13}$$

Then by knowing the regression coefficients of the bias a priori $\boldsymbol{\beta} = \hat{\boldsymbol{\beta}}$, the unknown parameters in Eqn. (8) which are the weights of RBFN can be calculated by

$$\boldsymbol{\lambda} = \boldsymbol{A}^{-1} (\hat{\boldsymbol{f}} - \boldsymbol{B}\hat{\boldsymbol{\beta}}). \tag{14}$$

The proposed method eliminates any need of imposing the extra orthogonality condition in Eqn. (9) . In order to evaluate the accuracy of this method, a comprehensive comparative study using several test functions has been done. The result of the study which compares our approach with the classic RBFN (5) and RBFN with a posteriori bias (10), by using several accuracy measures and error estimations, proves a slightly better performance and accuracy in addition to simplicity of the aforementioned approach to the other two.

The accuracy evaluation of the resulting surrogate model is done by using two different error measures: 1) the standard statistical analysis, and 2) the predicted residual sum of squares (PRESS). The standard statistical parameters used for validating the metamodel are root mean square error (RMSE), maximum absolute error (MAE) and coefficient of multiple determination or R square value (R^2). These parameters are in some extent dependent to each other and they are defined as follows:

$$\begin{aligned} \text{RMSE} &= \sqrt{\frac{\sum_{i=1}^{n} \left[\hat{f}_i - f_i\right]^2}{n}}, \\ \text{MAE} &= max|\hat{f}_i - f_i|, i = 1, ..., n, \\ R^2 &= 1 - \frac{SSE}{SST}, \end{aligned} \tag{15}$$

where n is the number of test points selected to evaluate the model, SSE is the sum of square errors, and SST is the total sum of squares calculated as

$$\begin{aligned} \text{SSE} &= \sum_{i=1}^{n} \left[\hat{f}_i - f_i\right]^2, \\ \text{SST} &= \sum_{i=1}^{n} \left[\hat{f}_i - \bar{f}\right]^2, \end{aligned} \tag{16}$$

where $\hat{f}_i$ is the observed (actual) function value at the i_{th} test point, f_i is the predicted function value at the i_{th} design point,

and $\bar{f}$ is the mean of observed function values at the test points. RMSE measures the global accuracy of the surrogate model, while MAE is used to evaluate the local performance of the model.

The predicted residual sum of squares or prediction error sum of squares (PRESS) is another method of measuring the accuracy of a metamodel [22]. The PRESS error is calculated by fitting the surrogate model to $n-1$ design points each time leaving out one design point which is used for testing the surrogate model.

The PRESS statistic defined as sum of squares of n PRESS residuals is calculated as

$$\text{PRESS} = \sum_{i=1}^{n} (e_i)^2 = \sum_{i=1}^{n} \left[\hat{f}_i - f_i\right]^2. \tag{17}$$

The two most common PRESS errors are root mean square PRESS denoted as RMSE_{PRESS} and $R^2_{prediction}$ calculated by

$$\text{RMSE}_{PRESS} = \sqrt{\frac{\text{PRESS}}{n}},$$

$$R^2_{prediction} = 1 - \frac{\text{PRESS}}{\text{SST}}. \tag{18}$$

Since the model recalculates the small residuals at each point, when they are not included in surrogate model, PRESS statistics are good measures of predictability of the surrogate model. It is obvious that the value of 0 for RMSE_{PRESS} and 1 for $R^2_{prediction}$ are the optimal desired values.

STRENGTH PARETO EVOLUTIONARY ALGORITHM (SPEA2)

SPEA2 is the improved version of the original SPEA by the same author [7], which addresses some potential weaknesses of SPEA. SPEA2 uses an initial population and an archive (external set). At the start, the random initial and archive population with fixed sizes are generated. The fitness value of each individual in the initial population and the archive population are calculated per iteration. Next, all non-dominated solutions of initial and external population are copied to the external set of next iteration (new archive). With the environmental selection procedure the size of the archive is set to a predefined limit. Afterwards, mating pool is filled with the solutions resulted by performing binary tournament selection on the new archive set. Finally, cross-over and mutation operators are applied to the mating pool and the new initial population is generated. If any of the stopping criteria is satisfied the non-dominated individuals in the new archive forms the Pareto optimal set.

The overall algorithm of SPEA2 is as follows [8]:

Algorithm (SPEA2 Main Loop)

Input : N (population size)
$\overline{N}$ (archive size)
T (maximum number of generations)
Output: A (non-dominated set)

Step 1: *Initialization*: an initial population P_0 and an archive (external set) $\overline{P}_0$ are generated. Set $t = 0$.

Step 2: *Fitness assignment*: Fitness values of the individuals in P_t and $\overline{P}_t$ are calculated.

Step 3: *Environmental selection*: All non-dominated individuals in P_t and $\overline{P}_t$ shall be copied to $\overline{P}_{t+1}$. If size of $\overline{P}_{t+1}$ exceeds $\overline{N}$, reduction of $\overline{P}_{t+1}$ is achieved by means of the truncation operator, otherwise $\overline{P}_{t+1}$ is filled with dominated individuals in P_t and $\overline{P}_t$, if size of $\overline{P}_{t+1}$ is less than $\overline{N}$.

Step 4: *Termination*: If $t > T$ or another stopping criterion is satisfied then, the non-dominated individuals in $\overline{P}_{t+1}$ creates the output set A.

Step 5: *Mating Selection*: Binary tournament selection with replacement is performed on $\overline{P}_{t+1}$ in order to fill the mating pool.

Step 6: *Variation*: Recombination and mutation operators shall be applied to the mating pool and the resulting population is set to P_{t+1} . Increment generation counter $(t = t+1)$ and go to Step 2.

More details of the algorithm, fitness assignment and environmental selection methods can be found in the original study [8]. Extended versions of SPEA2 are proposed by [23] and [24]. Kukkonen [24] introduces a pruning method to reduce the size of a set of non-dominated solution to a pre-defined limit, while the maximum possible diversity is encountered. The SPEA2 was implemented in an in-house MATLAB code.

NUMERICAL RESULTS

In the current study, multi-objective optimization of the disc brake system described in previous sections is performed based on surrogate modeling. Latin hypercube sampling and the finite element model are used to obtain the sampling points and associated actual function values. Optimization of the disc brake is carried out during hard barking of a truck for 20 seconds. The problem consists of three objective functions: (i) minimizing the maximum temperature of disc brake $(T_{max})[^{\circ}C]$, (ii) maximizing the brake energy during braking $(E_{brake})[Nm]$, and (iii) minimizing the mass of back plate $(m)[gr]$. The two first objectives are obtained from the finite element simulation results and the mass

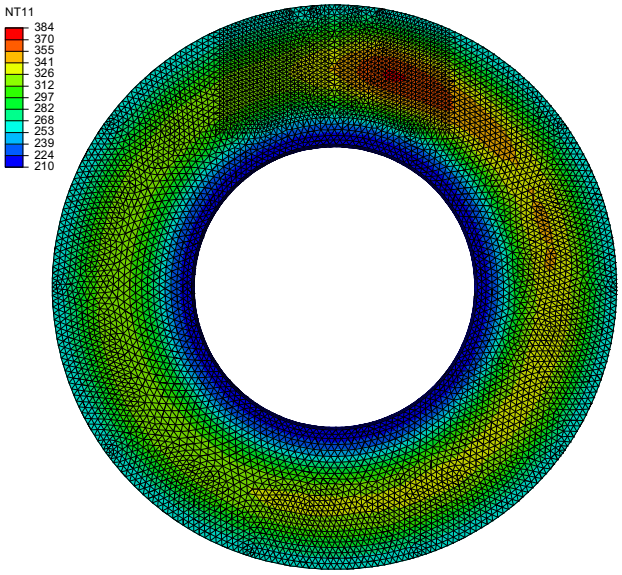

FIGURE 3. THE HEAT BAND ON THE DISC FOR A RANDOMLY SELECTED SOLUTION FROM THE PARETO FRONT.

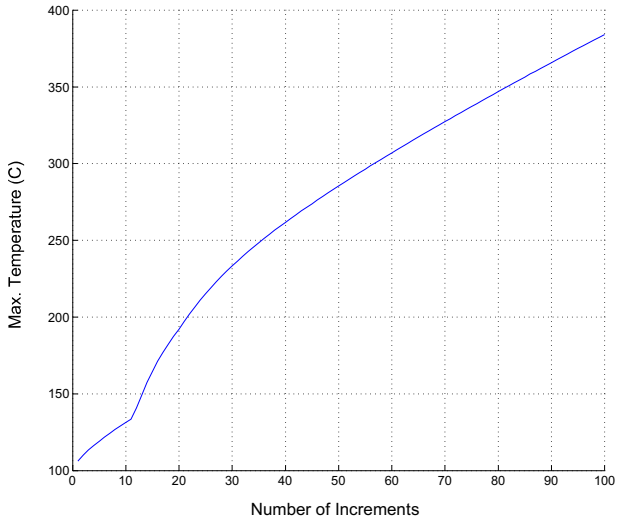

FIGURE 4. MAXIMUM TEMPERATURE-TIME PLOT FOR A RANDOMLY SELECTED SOLUTION FROM THE PARETO FRONT.

of back plate has a linear relation with thickness of back plate

$$m = \rho A t, \tag{19}$$

where $\rho = 7.8E{-}3[gr/mm^3]$ is the density of back plate material, $A = 2.0135E{+}4[mm^2]$ is the area of back plate calculated from the CAD model, and $t\,[mm]$ is the thickness of back plate which is one of the variables. The related design variables are: (i) the applied load during braking $(F)[N]$, (ii) type of material used for the brake pad represented by Young's modulus of brake pad $(E)[N/m^2]$, and (iii) thickness of back plate $(t)[mm]$. All the variables are limited within a design space. The overall formulation of the optimization problem is

$$\begin{aligned} \text{Minimize} \quad & T_{max}(\boldsymbol{x}), \\ \text{Maximize} \quad & E_{brake}(\boldsymbol{x}), \\ \text{Minimize} \quad & m(t), \\ & 17.15E+3 \le F \le 24.5E+3 \\ & 2.2E+8 \le E \le 2.2E+9,\ 5 \le t \le 14, \end{aligned} \tag{20}$$

where $\boldsymbol{x} = [F, E, t]$ is the vector of design variables. All the variables are linearly normalized between 0 and 1. The first two objective function values corresponding to a particular design variable is attained through the computationally expensive thermo-mechanical finite element analysis described previously, and the third objective function value is calculated by using Eqn. (19). 3

Iterative Latin hypercube sampling method using maximin (maximize minimum distance between points) with 20 iterations is used to select the the total of 200 design of experiments. In order to avoid generating 200 different CAD models manually, one for each thickness, 10 different thickness from $5[mm]$ to $14[mm]$ $(5, 6...14)$ are selected which for each thickness 20 sampling points are created by using the Latin hypercube function (LHSDESIGN) in MATLAB. Three separate work stations were simultaneously used to run the finite element simulations, one thickness at a time and the total 20 DoE of each thickness consumed approximately $120,000$ seconds of computation time. Therefore, all 200 simulations was completed at around 5 days.

Figure 3 illustrates the heat band on the surface of the disc brake generated from the finite element model, for one random solution selected from the Pareto front. The maximum temperature in terms of number of increments used in the finite element simulation, for the the same randomly selected point is plotted in Fig. 4.

All of the total 200 sampling points and their related objective function values are used to construct two surrogate models for the first two objectives, by employing the RBFN with a priori bias method.

The two error measures mentioned before are used to evaluate and select an accurate metamodel. Also, the most accurate radial basis function in Eqn. (6) with the lowest errors is identified. First, in order to measure the statistical errors using Eqn. (15), 3 of the sampling points are randomly chosen as test points. The surrogate model is fitted at the other 197 remaining

TABLE 1. STATISTICAL ERRORS OF MAXIMUM TEMPERATURE AND BRAKE ENERGY FOR ALL FOUR RADIAL BASIS FUNCTIONS.

Basis Function	Errors	Max Temp.	Brake Energy
Linear	$RMSE_{Mean}$	1.924	9.792
	$RMSE_{Max}$	6.045	46.551
	MAE_{Mean}	3.046	15.216
	MAE_{Max}	10.205	79.378
	R^2_{Mean}	0.979	1.000
Cubic	$RMSE_{Mean}$	**0.930**	**5.418**
	$RMSE_{Max}$	**3.431**	**37.906**
	MAE_{Mean}	**1.461**	**8.609**
	MAE_{Max}	**5.915**	**65.509**
	R^2_{Mean}	**0.997**	**0.999**
Guassian	$RMSE_{Mean}$	1.096	7.537
	$RMSE_{Max}$	4.401	159.706
	MAE_{Mean}	1.728	11.125
	MAE_{Max}	7.568	195.534
	R^2_{Mean}	0.986	1.000
Quadratic	$RMSE_{Mean}$	1.261	8.523
	$RMSE_{Max}$	4.251	117.823
	MAE_{Mean}	2.007	13.749
	MAE_{Max}	7.295	203.957
	R^2_{Mean}	0.989	0.998

TABLE 2. PRESS ERRORS OF MAXIMUM TEMPERATURE AND BRAKE ENERGY FOR ALL FOUR RADIAL BASIS FUNCTIONS.

Basis Function	PRESS Errors	Max Temp.	Brake Energy
Linear	RMSE_{PRESS}	1.914839	12.933808
	$R^2_{prediction}$	0.997377	0.999974
Cubic	RMSE_{PRESS}	1.504371	9.817290
	$R^2_{prediction}$	0.998381	0.999985
Guassian	RMSE_{PRESS}	**1.441460**	**7.981399**
	$R^2_{prediction}$	**0.998513**	**0.999990**
Quadratic	RMSE_{PRESS}	1.550602	9.345428
	$R^2_{prediction}$	0.998280	0.999986

DoE, and the statistical errors (RMSE, MAE and R^2) is calculated at the 3 sampling test points. Furthermore, to avoid any probable sensitivity of metamodel to a specific DoE, the above procedure is repeated 100 times, for each run 3 different test points, consequently 197 training points are randomly selected and the errors are calculated. Finally, the average of all 100 sets of errors $(RMSE_{Mean}, MAE_{Mean}, R^2_{Mean})$, the maximum RMSE $(RMSE_{Max})$ and the maximum MAE (MAE_{Max}) of all 100 error sets are used for evaluation. The aforementioned errors for all basis functions in Eqn. (15), are shown in Tab. 1.

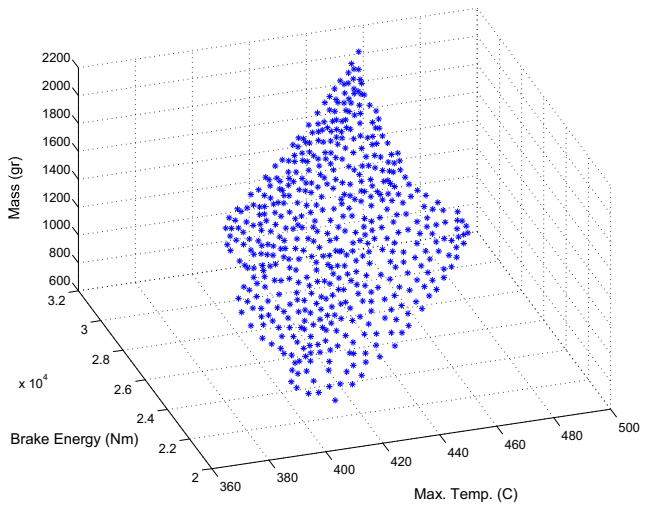

FIGURE 5. THE PARETO FRONT IN OBJECTIVE SPACE FOR THE THREE OBJECTIVES.

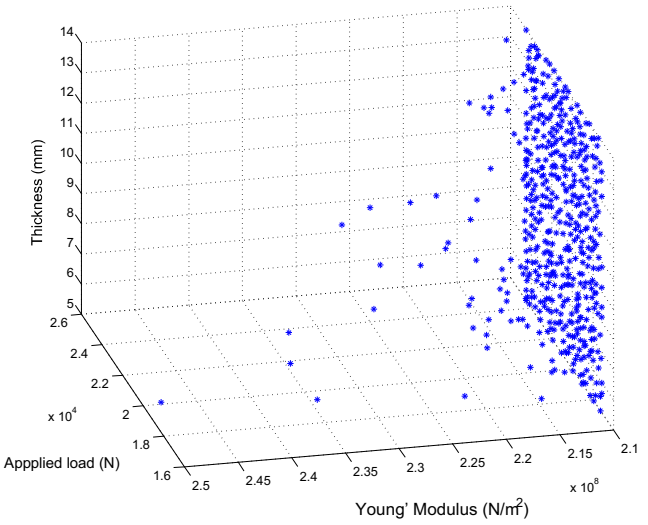

FIGURE 6. THE PARETO FRONT IN DECISION VARIABLE SPACE FOR THE THREE VARIABLES.

Since the third objective function follows a linear mathematical relation (Eqn. 19), there is no need to perform an error analysis for this specific objective.

Next, the PRESS errors (RMSE_{PRESS} and $R^2_{prediction}$) are calculated for all basis functions in Eqn. (15) by using Eqn. (18).

The results are presented in Tab. 2 to evaluate the accuracy of overall metamodeling technique and each basis function. The shape parameter for all basis functions is set to one ($\gamma = 1$).

The results of statistical error analysis presented in Tab. 1 and the calculated PRESS errors shown in Tab. 2, clearly shows an acceptable overall performance of our meta-modelling approach regardless of the type of radial basis function. In the worst case of statistical errors, the maximum deviation for the first objective, which is the maximum temperature, is $10.2[^{\circ}C]$ (5.8%) related to linear basis function, and the maximum absolute error (MAE_{Max}) for the second objective, which is brake energy, is $203.9[Nm]$ (2.2%) related to quadratic basis function. The RMSE and MAE errors for both of objectives compared to the range of each objective ($T_{Max} = 176[^{\circ}C]$, $E_{brake} = 9053[Nm]$), approves the perfect fit of our metamodeling technique. Furthermore, the very near value of R^2 and $R^2_{prediction}$ to 1 confirms the good performance of the metamodeling approach. The boldface values in Tab. 1, which are related to cubic basis function, are the lowest statistical errors among the four basis functions. Likewise, PRESS error values for Gaussian basis function, boldfaced in Tab. 2, indicates the better prediction of Gaussian among other three basis functions. However, the difference between PRESS errors related to Gaussian and cubic basis function, where Guassian has the lower error values, is very small, while this difference in statistical errors, where cubic basis function is the superior, is rather considerable. Therefore we decided to use the cubic basis function in this study.

Multi-objective optimization of problem is solved by coupling the SPEA2 algorithm with the two constructed metamodels and the mass formulation with the following parameter values:

Initial population size: 500
External set population size: 500
Cross over probability: $0.7 \sim 0.95$
SBX Crossover distribution index [25]:$2 \sim 15$

Above parameter was selected by experience by applying SPEA2 algorithm on different test functions, which showed the best results. To be sure of the optimality of obtained solutions, the SPEA2 optimization algorithm was run for 10 times, each run with randomly chosen parameter values within the ranges mentioned above. After, all of the 10 sets of non-dominated solutions were combined and the best set of non-dominated solutions was found and reported as the Pareto optimal set of problem.

The final Pareto optimal set including the 500 non-dominated solutions was obtained from the overall 5000 non-dominated solutions generated from the 10 multi-objective optimization runs. The final non-dominated solutions creates the Pareto front shown in Fig. 5. The Pareto front indicates a surface covering all possible mass values. In order to better analyse and understand the results of the multi-objective optimization, the Pareto front in decision variable space is also shown in Fig. 6. However, the $3D$ plot used to present the Pareto front for the three objectives, which each axes represents one objective, can be confusing and vague. Researchers [26, 27] suggested using scatter-plot matrix to illustrate the relation between the objective functions, also to compare different optimization algorithms for identical problems.

In engineering applications, same as our problem in this article, the relation of variables with objective functions and the non-dominated solutions in variable space is an imperative issue. Investigating the variations of each variable of non-dominated solutions and the effect of the variations to the objective functions and other variables can be very helpful in better understanding the multi-objective optimized problem. Here in Fig. 7, an extended version of scatter-plot matrix is employed to show these variations and their affects. For this purpose, each of the three variables and the three objective functions are marked in the diagonal plots of a 6×6 scatter-matrix plot. The off-diagonal plots clearly illustrate the non-dominated solutions in objective and variable space.

The Pareto front in variable space and the second column of the scatter-plot matrix clearly indicate that a brake pad with lowest possible stiffness $(2.1E+8[N/m^2])$ will result in an optimized solution with regards to all three objectives. However, the vertical surface of the Pareto front in Fig. 6 and the surfaces in first and third column of the scatter-plot matrix reveals that a designer can choose a trade-off solution from the non-dominated optimal set according to the preference of the objectives. Also, the linear relation of thickness and mass can be seen in plot(3,5) of the scatter-plot matrix. Another interesting aspect of the multi-objective optimization results which is revealed in plot(1,4) of Fig. 7 is the linear relation of applied braking load and brake energy. Therefore, by applying more load during braking the brake energy will increase. On the other hand, the increase in applied load will result in a higher temperature in the disc brake, shown in plot(1,3) of Fig. 7, creating a trade-off situation for the designer. Although the Pareto front between the thickness of back plate and maximum temperature illustrated in plot(3,3) is a surface, the slope depicts an overall decrease in maximum temperature with an increase in thickness.

From the final non-dominated solutions it can be seen that the maximum temperature ranges from $369.82[^{\circ}C]$ to $490.61[^{\circ}C]$ and the brake energy is between $2.124E+4[Nm]$ and $3.049E+4[Nm]$. If a designer's main objective is to have the lowest possible mass for the back plate with the value of $785.3[gr]$, the maximum temperature will range from $409[^{\circ}C]$ to $490.6[^{\circ}C]$ and the brake energy will be limited between $2.146E+4[Nm]$ and $3.044E+4[Nm]$, while a back plate with the maximum possible mass of $2199[gr]$ will change the range of maximum temperature and brake energy from $379[^{\circ}C]$ to $447[^{\circ}C]$ for the first and from $2.153E+4[Nm]$ to $2.978E+4[Nm]$ for the latter. Thus, with a compensation of $30[^{\circ}C]$ increase in maximum temperature or $70[Nm]$ decrease in brake energy, one can reduce the mass of the back plate upto $1414[gr]$, resulting to a great amount of cost

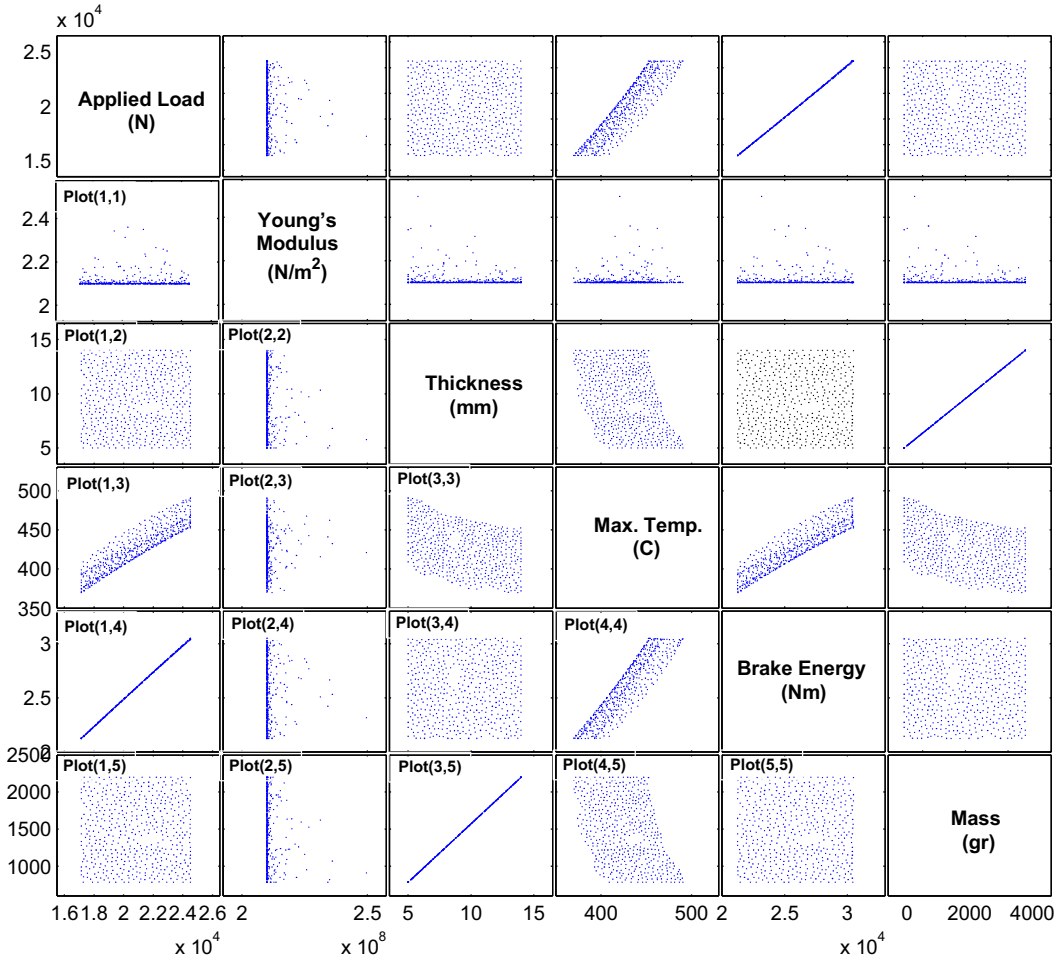

FIGURE 7. THE SCATTER-MATRIX PLOT INCLUDING THE THREE VARIABLES AND THE THREE OBJECTIVES.

reduction in back plate material. Other similar cases can be investigated and analysed from figures 5, 6 and 7. Therefore an engineer or designer can select the best design variables which full-fill his/her objective desires by analysing the Pareto fronts, scatter-plot matrix and the set of non-dominated solutions.

CONCLUDING REMARKS

In this paper it is demonstrated that SPEA2 and RBFN with a priori bias are powerful tools for performing multi-objective optimization of multi-physics systems such as a disc brake system to a heavy truck. The maximum temperature generated on the disc, the brake energy of system and the mass of back plate of brake pad during a 20 second hard braking are optimized. The design variables are the applied load of braking, brake pad material (Young's modulus) and the thickness of back plate.

The results predicted the possibility of approximately $1.4[Kg]$ mass reduction with accepting $30[^{\circ}C]$ increase in maximum temperature and $70[Nm]$ decrease in brake energy. The plots and non-dominated solutions also recommended the use of a brake pad with lowest possible stiffness. Additionally, we found out that there are possibilities to reduce the maximum temperature upto $121[^{\circ}C]$ or increase the brake energy upto $9.25e^3[Nm]$ with a compensation on other objectives.

In future the multi-objective optimization of the disc brake can be studied with increasing the number of variables. In this study the braking time was fixed to 20 seconds, while considering the braking time as a new variable could lead to useful results. By extending the thermo-mechanical finite element analy-

sis to include the fatigue life of disc in the output of simulation, maximizing the fatigue life of disc could be an interesting topic contemplated for future works.

ACKNOWLEDGMENT

This project was financed by Vinnova (FFI-Strategic Vehicle Research and Innovation) and Volvo 3P.

REFERENCES

[1] Kao, T., Richmond, J., and Douarre, A., 2000. "Brake disc hot spotting and thermal judder: an experimental and finite element study". *International Journal of Vehicle Design,* ***23***(3), pp. 276–296.

[2] Dufrénoy, P., and Weichert, D., 2003. "A thermomechanical model for the analysis of disc brake fracture mechanisms". *Journal of Thermal Stresses,* ***26***(8), pp. 815–828.

[3] Hee, K., and Filip, P., 2005. "Performance of ceramic enhanced phenolic matrix brake lining materials for automotive brake linings". *Wear,* ***259***(7-12), pp. 1088–1096. cited By (since 1996) 36.

[4] Hong, U., Jung, S., Cho, K., Cho, M., Kim, S., and Jang, H., 2009. "Wear mechanism of multiphase friction materials with different phenolic resin matrices". *Wear,* ***266***(7-8), pp. 739 – 744.

[5] AbuBakar, A.R., O. H., 2008. "Wear prediction of friction material and brake squeal using the finite element method". *Wear,* ***264***(11-12), pp. 1069–1076. cited By (since 1996) 11.

[6] Deb, K., Pratap, A., Agarwal, S., and Meyarivan, T., 2000. "A fast elitist multi-objective genetic algorithm: Nsga-ii". *IEEE Transactions on Evolutionary Computation,* ***6***, pp. 182–197.

[7] Zitzler, E., and Thiele, L., 1998. *An evolutionary algorithm for multiobjective optimization: The strength Pareto approach*. No. 43. Citeseer.

[8] Zitzler, E., Laumanns, M., and Thiele, L., 2001. "SPEA2: Improving the strength Pareto evolutionary algorithm". *Computer Engineering*, pp. 1–21.

[9] Knowles, J., 1999. "The pareto archived evolution strategy: A new baseline algorithm for pareto multiobjective optimisation". *Evolutionary Computation, 1999. CEC*.

[10] Knowles, J., 2000. "Approximating the nondominated front using the Pareto archived evolution strategy". *Evolutionary computation*, pp. 1–35.

[11] Corne, D., and Knowles, J., 2000. "The Pareto envelope-based selection algorithm for multiobjective optimization". *Problem Solving from Nature PPSN VI*(Mcdm).

[12] Corne, D., Jerram, N., and Knowles, J., 2001. "PESA-II: Region-based selection in evolutionary multiobjective optimization". *Genetic and Evolutionary*.

[13] Box, G. E. P., and Wilson, K. B., 1951. "On the experimental attainment of optimum conditions". *Journal of the Royal Statistical Society. Series B (Methodological),* ***13***(1), pp. 1–45.

[14] Sacks, J., Schiller, S. B., and Welch, W. J., 1989. "Designs for computer experiments". *Technometrics,* ***31***(1), pp. 41–47.

[15] Hardy, R. L., 1971. "Multiquadric equations of topography and other irregular surfaces". *Journal of Geophysical Research,* ***76(8)***, pp. 1905–1915.

[16] Vapnik, V., Golowich, S. E., and Smola, A., 1996. "Support vector method for function approximation, regression estimation, and signal processing". In Advances in Neural Information Processing Systems 9, Vol. 9, pp. 281–287.

[17] Haykin, S., 1998. *Neural Networks: A Comprehensive Foundation (2nd Edition)*, 2 ed. Prentice Hall, July.

[18] Simpson, T. W., 2008. "Desgin and analysis of computer experiments in multidisciplinary design optimization:A review of How Far We Have Come - or Not". pp. 1–22.

[19] Benseddiq, N., Weichert, D., Seidermann, J., and Minet, M., 1996. "Optimization of design of railway disc brake pads". *Proceedings of the Institution of Mechanical Engineers, Part F: Journal of Rail and Rapid Transit,* ***210***(1), pp. 51–61.

[20] Strömberg, N., 2011. "An Eulerian approach for simulating frictional heating in disc-pad systems". *European Journal of Mechanics - A/Solids,* ***30***(5), pp. 673 – 683.

[21] Krishnamurthy, T., 2003. "Response surface approximation with augmented and compactly supported radial basis functions". Vol. 5, pp. 3210–3224. cited By (since 1996) 0.

[22] Myers, R. H., Montgomery, D. C., and Anderson-Cook, C. M., 2009. *Response Surface Methodology: Process and Product Optimization Using Designed Experiments (Wiley Series in Probability and Statistics)*, 3 ed. Wiley, Jan.

[23] Kim, M., Hiroyasu, T., Miki, M., and Watanabe, S., 2004. "SPEA2+: Improving the performance of the strength Pareto evolutionary algorithm 2". *Parallel problem solving from . . .* , pp. 1–10.

[24] Kukkonen, S., 2006. "A fast and effective method for pruning of non-dominated solutions in many-objective problems". *Parallel Problem Solving from Nature-PPSN IX*, pp. 1–20.

[25] Deb, K., and Kumar, A., 1995. "Real-coded Genetic Algorithms with Simulated Binary Crossover: Studies on Multimodel and Multiobjective Problems". *Complex Systems,* ***9***(6), pp. 431–454.

[26] Meisel, W. L., 1973. "Tradeoff decision in multiple criteria decision making". *Multiple Criteria Decision Making*, pp. 461–476.

[27] Cleveland, W. S., 1994. *The Elements of Graphing Data*. Murry Hill,NJ: ATI&T Bell Laboratories.